

Technical Note

The Potential Use of Multi-Band SAR Data for Soil Moisture Retrieval over Bare Agricultural Areas: Hebei, China

Xiang Zhang ^{1,2}, Baozhang Chen ^{1,3,*}, Hongdong Fan ², Jilei Huang ¹ and Hui Zhao ⁴

Received: 3 November 2015; Accepted: 17 December 2015; Published: 23 December 2015

Academic Editors: Nicolas Baghdadi and Prasad S. Thenkabail

¹ School of Environment Science and Spatial Informatics, China University of Mining and Technology, Xuzhou 221116, China; zhangxiangcumt@126.com (X.Z.); 447168412@163.com (J.H.)

² Jiangsu Key Laboratory of Resources and Environmental Information Engineering, China University of Mining and Technology, Xuzhou 221116, China; cumtfanhd@163.com

³ Jiangsu Center for Collaborative Innovation in Geographic Information Resource Development and Application, Nanjing 210023, China

⁴ National Geomatics Center of China, Beijing 100080, China; zhaohui@nsdi.gov.cn

* Correspondence: baozhang.chen@igsnr.ac.cn; Tel.: +86-158-1117-2369

Abstract: The potential use of TerraSAR-X and Radarsat-2 data for soil moisture retrieval over bare agricultural areas was investigated using both empirical and semi-empirical approaches. For the empirical approach, the Support Vector Regression (SVR) model was used with two cases: (1) using only one C-band or X-band image; and (2) using a pair of C-band and X-band images jointly. For the semi-empirical approach, the modified Dubois model based on C-band and X-band SAR data was developed to estimate soil moisture content. The experiments were implemented over two bare agricultural areas, and *in-situ* measurements were carried out to assess the methods. The results showed that the TerraSAR-X and Radarsat-2 are suitable remote sensing tools for the estimation of surface soil moisture, with an accuracy of about 3 vol % (root mean square error, RMSE) over bare agricultural areas. Compared with the results obtained by Radarsat-2 data, TerraSAR-X data gives a slight improvement in estimating soil moisture. The accuracy of the soil moisture estimation was improved further when the two bands SAR data were used (RMSE of about 2.2 vol %) instead of only one. Moreover, the modified Dubois model showed comparable accuracy to the empirical model independent of the surface roughness.

Keywords: soil moisture; TerraSAR-X; Radarsat-2; SVR; Dubois model

1. Introduction

Soil moisture content is an important parameter in the Earth surface water cycle and energy exchange. Remote sensing techniques allow soil moisture to be detected over large areas. Therefore, considerable efforts have been devoted to the application of active microwave remote sensing to monitor surface soil moisture [1–6]. Among active microwave remote sensing techniques, Synthetic Aperture Radar (SAR) is a potential technique for the estimation of soil moisture content with suitable temporal and spatial resolution. The SAR return signal from a bare soil surface is mainly determined by sensor configuration parameters (frequency, polarization, and incidence angle) and soil surface parameters (dielectric constant and surface roughness) [7,8]. Therefore, the extraction of reliable soil moisture information from SAR data is subject to the efficient modeling of the contribution of soil moisture and surface roughness to the backscattering information.

A number of approaches have been proposed, and different results have been obtained with different model parameters, such as vegetation cover and soil surface roughness [9–11]. These

parameters complicate the estimation of soil moisture from SAR data, obviously producing deviation in the estimation results. Among others, three main methods for soil moisture inversion have been developed in the literature: empirical regression technique [12], semi-empirical model [13,14], and theoretical model [15–18]. Notarnicola *et al.* [19] compared the Bayesian and neural network approaches for soil moisture inversion. The Bayesian and neural network methods showed similar capability in estimating soil dielectric constant. The error of the Bayesian method increases if the number of input parameters increases, whereas, for the neural network method, the error decreases with an increase in the number of input parameters. Said *et al.* [20] used an artificial neural network with multiple input parameters to estimate soil moisture content. The neural network inversion was better than the multiple regression approach. Paloscia *et al.* [21] compared the artificial neural network approach, Bayesian approach, and Nelder-Mead direct-search method for soil moisture inversion using ASAR data and simulated data. The results showed that artificial neural network is the most practical method, which gives the optimal compromise among the accuracy, stability, and speed in estimation of soil moisture. Pasolli *et al.* [22,23] introduced Support Vector Regression (SVR) model into soil moisture inversion using microwave remote sensing data. The performance of the SVR model was compared with that obtained by a multilayer perceptron (MLP) neural network. The results indicated that the SVR model is a valid alternative to the MLP neural network regression model, and the SVR model is more stable and robust to the noise and outliers in the data.

Among the numerous soil surface scattering models in the literature, the widely-used models are two semi-empirical models, the Oh model and the Dubois model, and a theoretical model, the Integral Equation Model (IEM) [24]. Semi-empirical models establish relatively simple relationships between soil surface characteristics and SAR backscattering coefficients which reflect to a certain extent physical mechanism of the scattering targets. Nevertheless, they depend on several parameters which are generally site specific and therefore valid for limited soil surface conditions. Oh developed an experimental relationship relating the ratios of backscattering coefficients in different polarizations to soil dielectric constant and surface roughness. Dubois *et al.* linked co-polarization backscattering coefficients to soil dielectric constant and surface roughness. Rao *et al.* [25] used the Dubois model to estimate soil moisture based on HH and HV polarization backscattering coefficients. The surface roughness parameter was replaced by a linear regression model derived by linking the root mean square (RMS) height to the cross polarization ratio. Sahebi and Angles [26] modified the Dubois model to estimate soil moisture content using single polarization backscattering coefficient with two incidence angles, and the results showed good agreement with the measured soil moisture. Chai *et al.* [27] combined the water cloud model and Dubois model to estimate soil moisture in plateau pasture regions using polarimetric Radarsat-2 data. The surface roughness effect was eliminated by solving the Dubois equations. Validation results indicated that the developed Dubois model with minimum prior knowledge needed is the appropriate soil moisture estimation approach for the challenging environment. Theoretical models are based on electromagnetic scattering theory, which can establish site-independent relationships between the backscattering coefficients and the soil parameters. Thus, theoretical models are more suitable for estimating soil moisture over varying landscapes. However, these models are mathematically more complex and involve numerous parameters and heavy computational burden [28]. As a consequence, the complexity of theoretical models restricts their application.

Another widely used method is the change detection technique. The main principle of this approach is that the temporal variation of vegetation and surface roughness generally occurs over a longer time scale than soil moisture [29]. Therefore, multi-temporal SAR data can minimize the effect of surface roughness and vegetation. Thus, the relationships between the changes of backscattering coefficients and changes in soil moisture can be established. These theories have been widely used with different retrieval techniques and SAR data [30–33].

With the increasing availability of SAR data, more emphasis is being focused on the estimation of soil moisture from multi-configuration SAR data, which is promising in decoupling the surface

roughness and vegetation contribution from the retrieval procedure. Thus, it is likely to overcome the difficulty of soil moisture inversion under complex environmental conditions. Multi-incidence angle [34], multi-polarization [35,36] and multi-frequency [37] SAR data have been used to estimate soil moisture for different environments. The significant advantage of multi-incidence angle SAR data is the ability to quantify surface roughness without in-situ measurements [38]. Baghdadi *et al.* [39] investigated soil moisture inversion using ASAR data with low and high incidence angles. The results of the soil moisture inversion were improved significantly by using both incidence angles data instead of only one. Compared to the results obtained by high incidence angle SAR data, the use of low incidence angle data resulted in a distinct improvement in soil moisture inversion. Multiple polarization SAR allows for the simultaneous acquisition of backscattering information with two or four polarimetric modes and provides great potential for soil moisture inversion. By decomposing the polarimetric response, the corresponding contributions of vegetation cover and soil surface can be separated [40,41]. The soil moisture content can be estimated via the polarimetric parameters representing the soil surface characteristics [42]. Therefore, multi-configuration SAR data are promising for soil moisture inversion under different soil conditions.

The objective of this study is to investigate the potential of soil moisture inversion using multi-band space-borne SAR data (approximately simultaneous acquisition with HH polarization) over bare agricultural areas. The Radarsat-2 and TerraSAR-X data were acquired to provide different backscattering coefficients characterizing the soil surface. The SVR model was used to evaluate the potential of C-band and X-band SAR data for soil moisture inversion. Moreover, the Dubois model was modified to estimate soil moisture with the application of single polarization Radarsat-2 and TerraSAR-X data.

2. Study Area and Datasets

2.1. Study Area

The study area (Figure 1) is located at HanDan in Hebei Province, China ($114^{\circ}6'–114^{\circ}18' E$, $36^{\circ}26'–36^{\circ}38' N$). *In situ* measurements were implemented over the Jiulong ($114^{\circ}16' E$, $36^{\circ}27' N$) and Wannian ($114^{\circ}9' E$, $36^{\circ}37' N$) experimental areas, shown in Figure 1; both experimental areas are agricultural areas and relatively flat. During the period of SAR acquisitions (April 2015), the dominating crop was wheat, which covered approximately 20% of the agricultural area. The remaining soil surface was mainly bare plowed or unplowed soil awaiting future cultivation (corn). Therefore, we focused on soil moisture retrieval over bare agricultural areas.

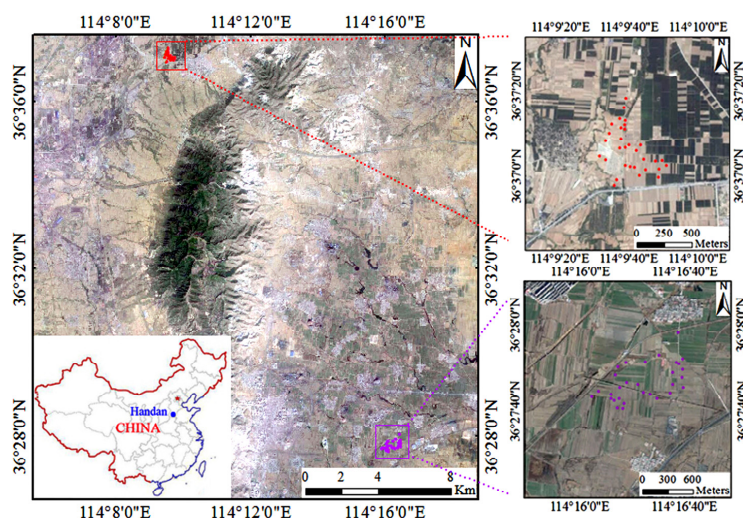


Figure 1. Study area and sampling sites. The upper right and lower right figures represent the Wannian and Jiulong experimental areas, respectively. The round dots indicate the sampling sites.

2.2. SAR Datasets

The Radarsat-2 and TerraSAR-X data were acquired over the study area, and the detailed information of the SAR data are shown in Table 1.

Table 1. Detailed information of the SAR data.

SAR Data	Acquisition Date	Band	Frequency	Polarization	Incidence Angle	Imaging Mode	Resolution
Radarsat-2	28 April 2015	C	5.3 GHz	HH	36°	Multi-Look Fine	5 m
TerraSAR-X	29 April 2015	X	9.6 GHz	HH	26°	StripMap	3 m

The Next ESA SAR Toolbox (NEST, [43]) was utilized to extract the backscattering coefficients. A Lee filter with 5×5 window was used to suppress the speckle noise. The data obtained were geocoded using a digital elevation model with 30-m resolution. Accurate geographical registration between the SAR data and field measurement sites was achieved through ten corner reflectors located in the experimental areas.

2.3. Field Measurements

Simultaneously with the acquisition of Radarsat-2 and TerraSAR-X data, field measurements were implemented over two experimental areas on 28 and 29 April 2015. During this time, there was no precipitation, obvious temperature change or agricultural activity over the experimental areas. Therefore, the soil moisture and surface roughness are assumed to be constant on 28 and 29 April 2015. Two soil surface parameters were obtained, including soil moisture content (0–5 cm depth) and surface roughness.

For the Jiulong and Wannian experimental areas, 30 and 31 sampling sites were selected, respectively. These field measurements can be used to calibrate and validate the soil moisture inversion models. For each sampling site, three sampling points were selected as representative within an area of $30 \text{ m} \times 30 \text{ m}$. The distance among the sampling points is approximately 10 m. The average measurement of the three sampling points is regarded as the sampling site measurement. The soil moisture of each site is represented as the average of three samples measurements. Soil moisture was collected by a calibrated TDR (Time Domain Reflectometry) probe, and the measured soil moisture content data were corrected based on the gravimetric method. Due to partial irrigation over the Jiulong experimental area, the soil moisture changes obviously. The soil moisture content varied from $10.2\% \text{ cm}^3/\text{cm}^3$ to $28.6\% \text{ cm}^3/\text{cm}^3$. The soil moisture was relatively lower over the Wannian experimental area due to little precipitation, and the soil moisture content varied from $8.5\% \text{ cm}^3/\text{cm}^3$ to $20.3\% \text{ cm}^3/\text{cm}^3$. A Q5H global positioning system (GPS) was used to identify and register the sampling positions with 1 m accuracy. The surface roughness was measured using a needle profiler (1-meter long and with 1-centimeter sampling intervals) and a digital camera. At each sampling point four field photographs of the surface roughness were obtained, two of these photographs were parallel to the row direction and the others were perpendicular to the row direction. The RMS height (s) and correlation length (l) were calculated using a Matlab program. The value of s varied from 0.4 cm to 1.8 cm over the Jiulong experimental area, while in the Wannian experimental area, s varied from 0.3 cm to 1.6 cm.

3. Methodology

3.1. Empirical Model

A proper inversion technique is of great importance for soil moisture retrieval. The estimation of soil moisture from SAR data by means of empirical methods requires the development of experimental relationships between the backscattering coefficient (σ) and the measured soil moisture

(m_v). For each experimental area (Jiulong and Wannian), approximately 60% of the sampling sites are used as the calibration data sets, the rest of the sampling sites are used as the validation data sets.

In the case of using one SAR image characterized by one band (C-band or X-band), the retrieval model without taking into account the surface roughness is represented as follows:

$$\sigma = f(m_v, \lambda) \Rightarrow m_v = f'(\sigma) \quad (1)$$

The joint use of two bands SAR data can eliminate the effects of surface roughness and, thus, allows relating the backscatter coefficient to soil moisture only. For two images acquired with C-band and X-band, the estimation of soil moisture can be obtained:

$$\left. \begin{aligned} \sigma_C &= f_1(m_v, s, \lambda_C) \\ \sigma_X &= f_2(m_v, s, \lambda_X) \end{aligned} \right\} \Rightarrow m_v = f'(\sigma_C, \sigma_X) \quad (2)$$

where s denotes the RMS height. The surface roughness parameter also can be represented as Z_s [44] or Z_g [45], where the correlation length is involved. Equation (2) should be the same if the Z_s or Z_g parameters are used.

The empirical models represented in Equations (1) and (2) were established by the calibration data sets using the SVR model. The validation for the empirical models was implemented using the validation data sets (approximately 40% of the sampling sites of each experimental area).

The SVR model is a robust and promising nonlinear machine learning technology [46], which was introduced to estimate soil moisture using microwave remote sensing data [22,47,48].

When a continuous parameter y (e.g., the volumetric soil moisture) needs to be estimated, given a set $x = (x_1, x_2, \dots, x_n)$ of n features extracted from SAR data (e.g., backscatter coefficients), this can be represented as:

$$y = f(x) + b \quad (3)$$

where f represents the input-output mapping and b is a Gaussian random variable. The calculation of y corresponds to the problem of obtaining a function f' as close as possible to the true mapping f .

The objective of the SVR model is to obtain a function f' that approximates f . For this purpose, the original low-dimensional input domain is projected to a high-dimensional space. Then, f is approximated to a linear function:

$$f'(x) = \omega \cdot \Phi(x) + d \quad (4)$$

where ω denotes the weight vector of the approximation function, $\Phi(\cdot)$ is the projection function, and d is the bias.

The optimal linear function is obtained, based on the minimization of structural risk, which combines the training error and the model complexity. The first part is obtained according to a ε -insensitive loss function, where ε quantifies the tolerance to errors. Equivalently, the penalty can be represented by the nonnegative slack variables ξ and ξ^* . The second part of the cost function is represented by the Euclidean norm of weight vector ω . The cost function to minimize can be expressed as

$$\psi(\omega, \xi) = C \sum_{i=1}^N (\xi_i + \xi_i^*) + \frac{1}{2} \|\omega\|^2 \quad (5)$$

satisfying the following constraints:

$$\left\{ \begin{aligned} y_i - [\omega \cdot \Phi(x_i) + d] &\leq \varepsilon + \xi_i, \\ [\omega \cdot \Phi(x_i) + d] - y_i &\leq \varepsilon + \xi_i^*, \quad i = 1, 2, \dots, N \\ \xi_i, \xi_i^* &\geq 0, \end{aligned} \right. \quad (6)$$

C is a regularization parameter that adjusts the tradeoff between the tolerance to empirical errors and the complexity of the function f' .

The constrained optimization problem in Equation (5) can be solved by introducing Lagrange multipliers α_1 and α_i^* , leading to a unique solution. Based on the samples in the original input domain, the final estimation function can be represented as follows:

$$f'(x) = \sum_{i \in N} (\alpha_i - \alpha_i^*) k(x_i, x) + d \quad (7)$$

where $k(\cdot)$ is the kernel function that satisfies Mercer's theorem [49].

3.2. Modified Dubois Model

Dubois *et al.* proposed a semi-empirical model that characterizes the co-polarized backscatter coefficients σ as functions of dielectric constant ϵ , incidence angle θ , RMS height s , and wavelength λ .

$$\sigma_{HH} = 10^{-2.75} \left(\frac{\cos^{1.5}\theta}{\sin^5\theta} \right) 10^{0.028\epsilon \tan\theta} \lambda^{0.7} (k_s \sin\theta)^{1.4} \quad (8)$$

$$\sigma_{VV} = 10^{-2.35} \left(\frac{\cos^3\theta}{\sin^3\theta} \right) 10^{0.046\epsilon \tan\theta} \lambda^{0.7} (k_s \sin\theta)^{1.1} \quad (9)$$

where k is the wave number, represented as $k = 2\pi/\lambda$. The model is suitable for bare soil, and it gives optimal results for $ks \leq 2.5$ and $m_v \leq 0.35 \text{ cm}^3/\text{cm}^3$. The soil surface characteristics of the experimental areas satisfy the applicable conditions of the Dubois model.

In the Dubois model, the soil dielectric constant can be obtained with the effective surface roughness parameters as inputs for the single polarization SAR data. However, obtaining prior information of surface roughness enhances the difficulty of soil moisture inversion. To solve this problem, two different bands SAR data with HH polarization were acquired in this study. For each sampling site, two backscattering coefficients were obtained from the Radarsat-2 and TerraSAR-X data. Hence, the Radarsat-2 and TerraSAR-X backscattering coefficients can be represented by Equation (8) with the same surface roughness and soil moisture data as inputs. The surface roughness parameter can be eliminated. Thus, a function of soil dielectric constant and backscattering coefficients and SAR configuration parameters, independent of surface roughness, can be derived:

$$\epsilon = \frac{\log_{10}(\sigma_C/\sigma_X) + 1.5\log_{10}\left(\frac{\cos\theta_X}{\cos\theta_C}\right) + 3.6\log_{10}\left(\frac{\sin\theta_C}{\sin\theta_X}\right) + 0.7\log_{10}(\lambda_C/\lambda_X)}{0.028(\tan\theta_C - \tan\theta_X)} \quad (10)$$

where the subscripts C and X represent the C-band Radarsat-2 and X-band TerraSAR-X images, respectively.

Thus, the soil dielectric constant can be obtained via Equation (10) based on two bands SAR data independent of surface roughness. Subsequently, soil moisture content can be calculated using the empirical method proposed by Topp *et al.* [50], a function of volumetric soil moisture content and dielectric constant:

$$m_v = -0.053 + 0.0292\epsilon - 5.5 \times 10^{-4}\epsilon^2 + 4.3 \times 10^{-6}\epsilon^3 \quad (11)$$

4. Results and Discussion

4.1. Empirical Model Experiments

For the Jiulong data set, 30 samples were acquired, of which 20 random samples were selected to establish the model for soil moisture retrieval, and the remaining 10 samples were used to validate the model. For the Wannian data set, 31 samples were acquired, of which 20 random samples were selected to establish the model and the remaining 11 samples were used to validate the model. The SVR model was utilized to estimate the soil moisture content with C-band and X-band SAR data as inputs. The results are shown in Figure 2.

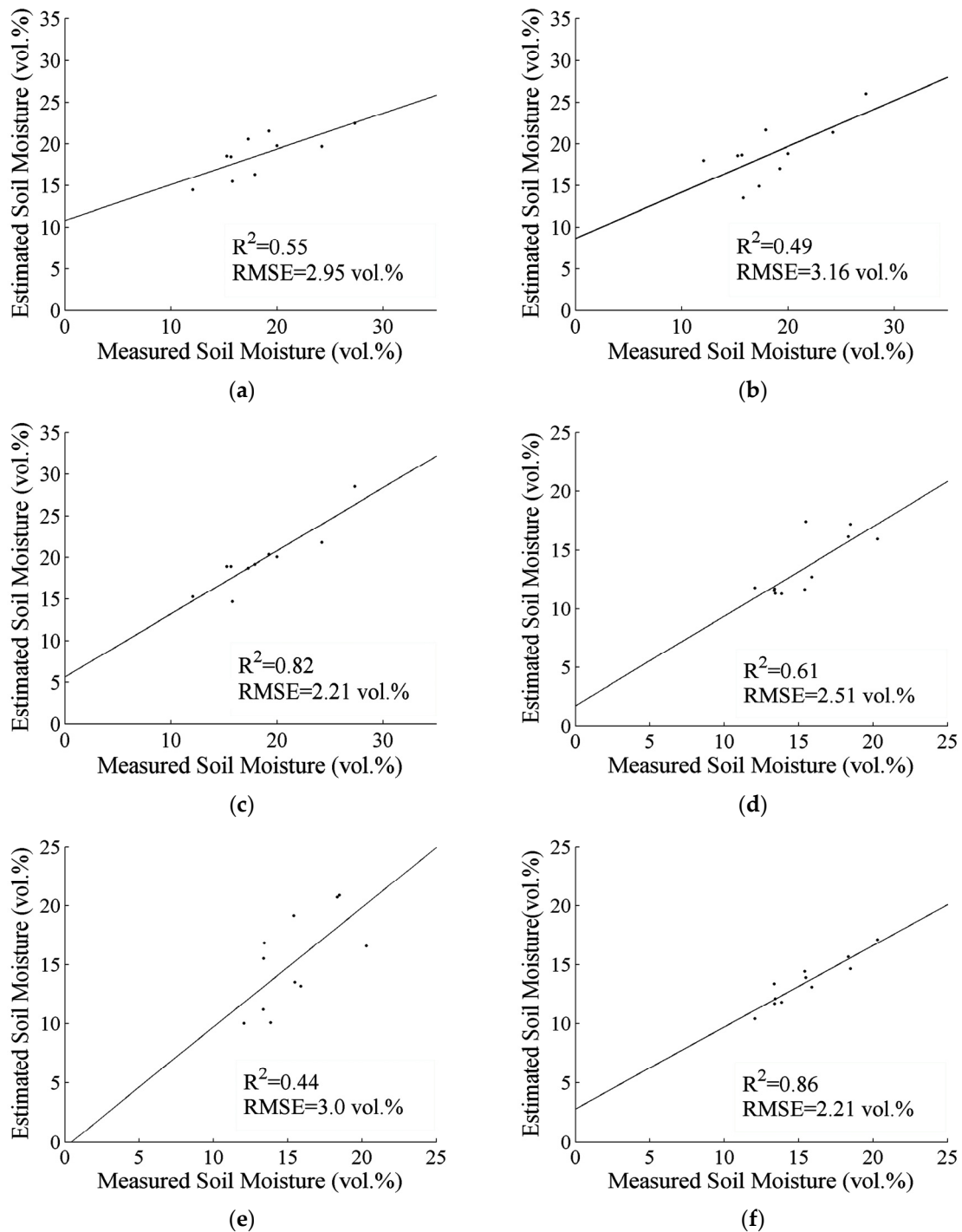


Figure 2. Comparisons between the measured and estimated soil moisture content using the SVR model: (a) Jiulong data set with TerraSAR-X ($R^2 = 0.55$, RMSE = 2.95 vol %); (b) Jiulong data set with Radarsat-2 ($R^2 = 0.49$, RMSE = 3.16 vol %); (c) Jiulong data set with TerraSAR-X and Radarsat-2 ($R^2 = 0.82$, RMSE = 2.21 vol %); (d) Wannian data set with TerraSAR-X ($R^2 = 0.61$, RMSE = 2.51 vol %); (e) Wannian data set with Radarsat-2 ($R^2 = 0.44$, RMSE = 3.0 vol %); and (f) Wannian data set with TerraSAR-X and Radarsat-2 ($R^2 = 0.86$, RMSE = 2.21 vol %).

Quantitative evaluation between the estimated and measured soil moisture were implemented. The Root Mean Square Error (RMSE), determination coefficient (R^2), Mean Relative Error (MRE), and Standard Deviation (SD) were selected as the indicators. The statistical results are shown in Table 2.

Table 2. Quantitative statistics between the measured and estimated soil moisture content using the SVR model.

Experimental Data Set	SAR Data	RMSE (cm ³ /cm ³)	R ²	MRE (%)	SD (cm ³ /cm ³)
Jiulong data set	TerraSAR-X	2.95	0.55	14.2	3.1
	Radarsat-2	3.16	0.49	17.4	3.28
	TerraSAR-X and Radarsat-2	2.21	0.82	12.3	1.93
Wannian data set	TerraSAR-X	2.51	0.61	14.0	1.78
	Radarsat-2	3.0	0.44	19.3	2.86
	TerraSAR-X and Radarsat-2	2.21	0.86	12.1	1.15

In the validation phase, the results obtained with the C-band SAR data showed an estimation error of about 3.2 vol % (RMSE) over the Jiulong experimental area. The use of X-band SAR gave slightly better results with an RMSE of about 3.0 vol %. For the Wannian experimental area, the results obtained with the C-band SAR data showed an estimation error of about 3.0 vol % (RMSE). The use of X-band SAR gave better results with an RMSE of about 2.5 vol %. The accuracy of the soil moisture estimation improved by using C-band and X-band SAR data together, with an RMSE of about 2.2 vol % over the Jiulong and Wannian experimental areas. Figure 2 shows the good agreement between the estimated and measured soil moisture over both experimental areas.

For the Jiulong and Wannian experimental areas, single band SAR data (C-band or X-band) gave accurate soil moisture estimation results (RMSE < 3.2%). The reason for this may be that the SVR model has good intrinsic generalization performance. Also, the SVR model is easy to handle and quick to train, and shows a good compromise between processing time and inversion accuracy. Thus, it is suitable for timeliness requirements [22,51]. Moreover, the SVR model is suitable for small training samples. For soil moisture inversion, extensive in-situ measurements are laborious and inefficient, and limited sampling sites can be obtained. The SVR model can solve this problem and, hence, is a suitable soil moisture inversion model.

Compared with the results obtained by Radarsat-2 data, the use of TerraSAR-X data provided an improvement in estimating soil moisture over the Jiulong and Wannian experimental areas. The C-band and X-band SAR data showed different sensitivity to soil surface roughness [52]. Smaller errors in the estimated soil moisture were obtained with the X-band SAR for a single incidence angle (RMSE of about 3 vol % for 26°, and 4 vol % for 52°) [53] than with the C-band SAR (RMSE of about 6 vol % for 20°, and 9 vol % for 40°) [39], where the surface roughness effect was not taken into account. When C-band SAR data with two incidence angles were used to estimate soil moisture content, where the surface roughness effect was reduced, the inversion results improved significantly over the single incidence angle C-band SAR data [39]. In contrast, the inversion accuracy of X-band SAR data with two incidence angles did not improve compared to the results of single incidence angle X-band SAR data [53]. This is due to the fact that the dependence of X-band SAR on surface roughness has been described as weak over agricultural areas [54,55]. Furthermore, Aubert *et al.* showed that the sensitivity of the X-band SAR data to soil moisture is significant [56]. Therefore, the single X-band SAR data obtained accurate soil moisture inversion results, even though the surface roughness was neglected in the inversion procedure.

Compared to the soil moisture inversion results using single X-band or C-band SAR, the X-band plus C-band SAR data for soil moisture inversion showed better results. The soil surface roughness is an important factor that influences soil moisture estimation using SAR data. For soil moisture inversion using the single X-band or C-band SAR data, the effect of surface roughness was not taken into account, which reduced the soil moisture estimation accuracy. In contrast, when the two bands SAR data were used to estimate soil moisture content, the surface roughness effect was reduced, which improved the accuracy of soil moisture inversion. When C-band SAR data with low and high incidence angles are combined to remove the effect of surface roughness, the soil moisture inversion accuracy improves significantly compared with only using the single incidence SAR data [39,57].

Moreover, the SAR signal is sensitive to soil properties in different ways and to a different extent depending on the SAR frequency [58], and the combination of SAR information acquired with different frequencies leads to a better characterization of the parameters affecting the SAR signal and thus to accurate estimation of the soil moisture. Therefore, the multi-band SAR data obtained satisfactory results over the Jiulong and Wannian experimental areas, owing to the elimination of surface roughness effect.

From the above analysis we can see that the SVR model with multi-band SAR data is effective for soil moisture inversion. The TerraSAR-X data obtained better results for soil moisture inversion over bare agricultural areas than Radarsat-2 data. However, X-band SAR is more sensitive to vegetation cover due to its weak penetration capability. Therefore, further study is needed for soil moisture inversion using X-band and C-band SAR over vegetation covered areas.

4.2. Modified Dubois Model Experiments

Soil surface roughness influences the radar backscattering response, which can result in biases in soil moisture inversion results. To overcome this difficulty, it is assumed that the soil surface roughness is constant during the period of SAR acquisition and in-situ measurements. Subsequently, solving the Dubois model with multi-band SAR data can eliminate the effect of soil surface roughness. Therefore, the soil dielectric constant can be calculated from Equation (10) with Radarsat-2 and TerraSAR-X backscattering coefficients and configuration parameters as inputs.

For the Jiulong and Wannian data sets, in-situ measured soil moisture was used to validate the modified Dubois model based on multi-band SAR data. Figure 3 represented the comparisons between the field measurements and estimated soil moisture obtained by the modified Dubois model.

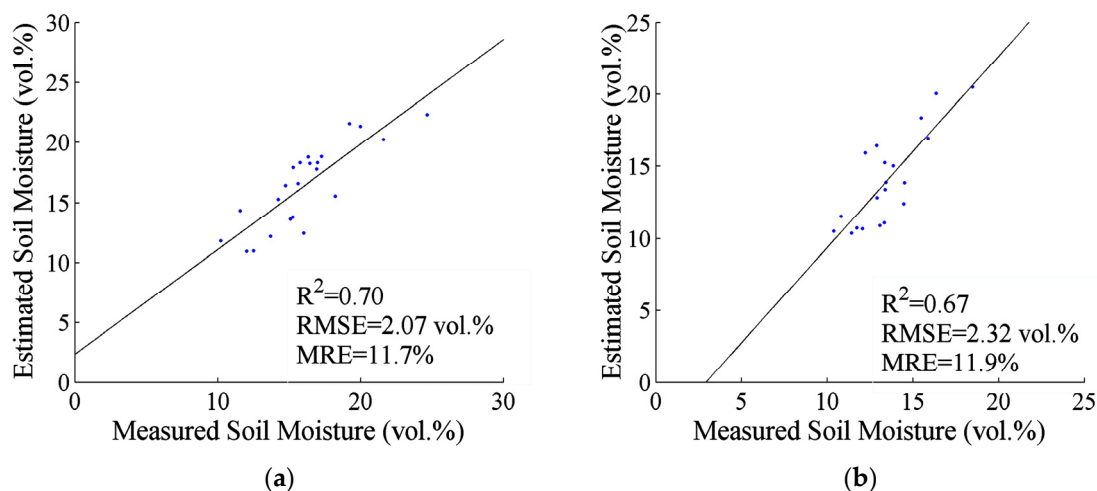


Figure 3. Comparisons between the measured and estimated soil moisture content using modified Dubois model: (a) Jiulong experimental area ($R^2 = 0.70$, $RMSE = 2.07$ vol %); (b) Wannian experimental area ($R^2 = 0.67$, $RMSE = 2.32$ vol %).

The modified Dubois model was used to estimate soil moisture based on the Radarsat-2 and TerraSAR-X data. The estimated soil moisture showed good agreement with measured soil moisture over the Jiulong (R^2 of about 0.7, $RMSE$ of about 2.1 vol %) and Wannian (R^2 of about 0.67, $RMSE$ of about 2.3 vol %) experimental areas.

Evaluation results indicated that the Dubois model based on multi-band SAR data is promising for soil moisture inversion over this study area. The estimated soil moisture showed good agreement with in-situ measurements in terms of accuracy and stability, owing to decoupling the effect of surface roughness from the SAR backscattering coefficient. The original Dubois model needs HH and VV polarization SAR data as inputs to estimate soil moisture content. Sahebi and Angles [26]

developed the Dubois model to estimate soil moisture content based on single polarization SAR data with two incidence angles. In this study, the modified Dubois model based on multi-band SAR data was developed and used to estimate soil moisture content independent of surface roughness. The results verified the efficiency of the developed Dubois model for soil moisture inversion over bare agricultural areas. Moreover, this method does not need prior knowledge of soil surface parameters.

Despite the accurate results were obtained, the multi-band space-borne SAR data are relatively difficult to acquire at present. This will limit the applications of multi-band SAR data for soil moisture inversion over large areas with frequent temporal coverage. However, with the development of space-borne SAR techniques, multi-band SAR data may be frequently acquired in the future, so the research of multi-band SAR data for soil moisture inversion is promising.

4.3. Comparison of Results

Evaluation results indicated that the SVR model and modified Dubois model based on Radarsat-2 and TerraSAR-X data are promising for soil moisture inversion over this study area. Therefore, the SVR model and modified Dubois model can be used to produce soil moisture maps on the basis of multi-band SAR data. Figure 4 shows the soil moisture content maps of the experimental areas.

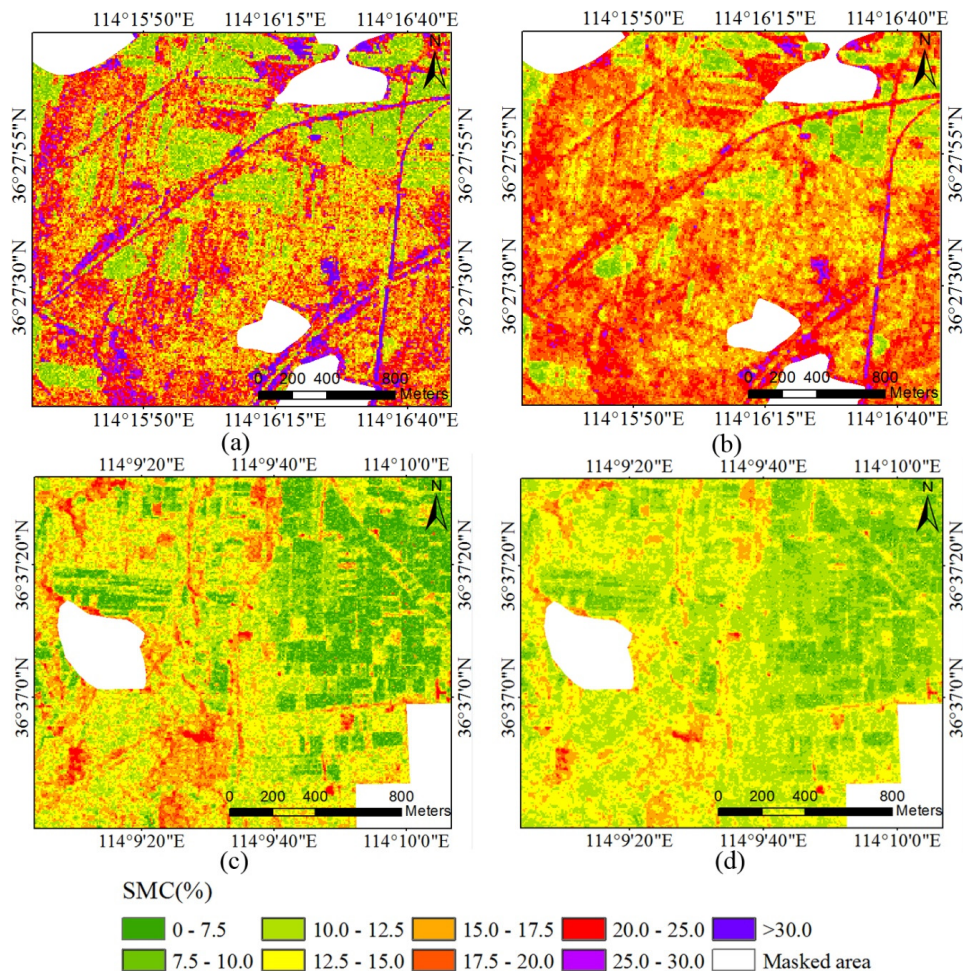


Figure 4. Soil moisture content maps of the Jiulong and Wannian experimental areas produced by the SVR model and modified Dubois model based on TerraSAR-X and Radarsat-2 data: (a) Jiulong experimental area with SVR model; (b) Jiulong experimental area with modified Dubois model; (c) Wannian experimental area with SVR model; and (d) Wannian experimental area with modified Dubois model. Rural areas are masked in white.

The results showed that the SVR model and modified Dubois model gave similar results for each of the experimental area. For the Jiulong and Wannian experimental areas, different land parcels showed different soil moisture content. The reason for this is that different land parcels correspond to different management measures, so the soil may be irrigated, plowed, or unplowed. Therefore, the soil moisture content varies between different land parcels. Correspondingly, the inversion results showed variations between different land parcels. The average soil moisture content over the Wannian experimental area was lower than over the Jiulong experimental area, which is in line with the field measurements. The difference of precipitation and soil texture between the experimental areas may be the cause of these results. Moreover, partial irrigation may also influence the distribution of the soil moisture.

The empirical and semi-empirical models were used to estimate regional soil moisture content on the basis of multi-band SAR data, and the accurate and reliable soil moisture content maps were obtained, which is significant in the application of hydrology, agronomy and climatology. The empirical model (SVR) based on multi-band SAR data gave accurate soil moisture inversion results for this study area. However, the applicability of this approach is restricted due to the limited representativeness of the soil conditions. The parameters of the modified Dubois model have a certain extent physical significance. Soil moisture content can be estimated using multi-band SAR data without prior information.

5. Conclusions

The main objective of this study is to investigate the potential of multi-band SAR data for soil moisture inversion over bare agricultural areas. The study tested the empirical model for soil moisture estimation from one band SAR data (C-band or X-band) and multi-band SAR data (both C-band and X-band). Additionally, the modified Dubois model based on multi-band SAR data was developed to estimate soil moisture content independent of surface roughness. The results of this study can be summarized as follows:

- (1) The retrieval algorithm performed well for single X-band and C-band SAR data. The results indicated that the TerraSAR-X and Radarsat-2 are suitable remote sensing tools for the estimation of surface soil moisture over bare agricultural areas.
- (2) Comparing with the results obtained by Radarsat-2 data, the TerraSAR-X data showed slightly higher accuracy for soil moisture inversion due to the weak sensitivity to surface roughness. The accuracy of the soil moisture estimation improved when two bands SAR data were used, owing to the decoupling of surface roughness effect from radar backscattering.
- (3) The modified Dubois model based on multi-band SAR data showed comparable accuracy with the empirical model independent of surface roughness. In areas where surface roughness parameters are not available, the model is promising.

Multi-band SAR data are promising for soil moisture retrieval over bare agricultural areas. Agricultural areas are seasonally covered with different crops, so further study is needed for soil moisture inversion using multi-band SAR data over vegetation covered areas. For this purpose, the simultaneous acquisition of multi-band SAR data is necessary. Therefore, the development of multi-band SAR satellite is promising for accurate land surface parameters inversion.

Acknowledgments: The authors wish to thank the ESA for providing the NEST software. The authors would like to thank Junkai Yang, Hua Chen, Chenliang Zhao, Xi Chen, Huifu Zhuang, Lei Wang, Da Li, Xiaoxiong Gao for their help with field measurements. This research was supported by the National Science Foundation of China (No. 41271116), Jiangsu Province: "double creation" program, the Basic Research Project of Jiangsu Province (Natural Science Foundation) (No. BK20130174), Ordinary University Graduate Student Scientific Research Innovation Projects of Jiangsu Province (No. KYLX_1393), the Priority Academic Program Development of Jiangsu higher education institutions (PAPD), and the Special Fund for Public Projects of National Administration of Surveying, Mapping, and Geoinformation of China (No. 201412016).

Author Contributions: Baozhang Chen designed the research. Xiang Zhang was responsible for the development of soil moisture inversion approaches. Xiang Zhang and Baozhang Chen wrote this paper. Hongdong Fan contributed to the analysis of the results. Jilei Huang and Hui Zhao participated in some data analysis and field experiments.

Conflicts of Interest: The authors declare no conflict of interest.

References

1. Ulaby, F.T.; Dubois, P.C.; van Zyl, J. Radar mapping of surface soil moisture. *J. Hydrol.* **1996**, *184*, 57–84. [[CrossRef](#)]
2. Mladenova, I.; Lakshmi, V.; Walker, J.; Long, D.; de Jeu, R. An assessment of QuikSCAT Ku-band scatterometer data for soil moisture Sensitivity. *IEEE Geosci. Remote Sens. Lett.* **2009**, *6*, 640–643. [[CrossRef](#)]
3. Mladenova, I.; Lakshmi, V. Terrain: Slope Influences on QuickSCAT Backscatter. *IEEE Trans. Geosci. Remote Sens.* **2009**, *47*, 2722–2732. [[CrossRef](#)]
4. Mladenova, I.; Lakshmi, V.; Walker, J.; Panciera, R.; Wagner, W.; Doubkova, M. Validation of the ASAR global monitoring mode soil moisture product using the NAFE'05 data set. *IEEE Trans. Geosci. Remote Sens.* **2010**, *48*, 2498–2508. [[CrossRef](#)]
5. Narvekar, P.S.; Entekhabi, D.; Kim, S.B.; Njoku, E.G. Soil moisture retrieval using L-band radar observations. *IEEE Trans. Geosci. Remote Sens.* **2015**, *53*, 3492–3506. [[CrossRef](#)]
6. Gorrab, A.; Zribi, M.; Baghdadi, N.; Mougenot, B.; Fanise, P.; Chabaane, Z.L. Retrieval of both soil moisture and texture using TerraSAR-X images. *Remote Sens.* **2015**, *7*, 10098–10116. [[CrossRef](#)]
7. Ulaby, F.T.; Bradley, G.A.; Dobson, M.C. Microwave backscatter dependence on surface roughness, soil moisture and soil texture, Part-II: Vegetation covered soil. *IEEE Trans. Geosci. Remote Sens.* **1979**, *17*, 33–40. [[CrossRef](#)]
8. Mattia, F.; Le Toan, T.; Souyris, J.C.; de Carolis, G.; Floury, N.; Posa, F.; Pasquariello, G. The effect of surface roughness on multifrequency polarimetric SAR data. *IEEE Trans. Geosci. Remote Sens.* **1997**, *35*, 954–966. [[CrossRef](#)]
9. Balenzano, A.; Mattia, F.; Satalino, G.; Davidson, M. Dense temporal series of C- and L-band SAR data for soil moisture retrieval over agricultural crops. *IEEE J. Sel. Top. Appl. Earth Obs. Remote Sens.* **2011**, *4*, 439–450. [[CrossRef](#)]
10. Lucas, R.; Armston, J.; Fairfax, R.; Fensham, R.; Accad, A.; Carreiras, J.; Kelley, J.; Bunting, P.; Clewley, D.; Bray, S.; *et al.* An evaluation of the ALOS PALSAR L-band backscatter-Above ground biomass relationship Queensland, Australia: Impacts of surface moisture condition and vegetation structure. *IEEE J. Sel. Top. Appl. Earth Obs. Remote Sens.* **2010**, *3*, 576–593. [[CrossRef](#)]
11. Kerr, Y.H. Soil moisture from space: Where are we? *Hydrogeol. J.* **2007**, *15*, 117–120. [[CrossRef](#)]
12. Lin, D.S.; Wood, E.F.; Bevan, K.; Saatchi, S. Soil moisture estimation over grass-covered areas using AIRSAR. *Int. J. Remote Sens.* **1994**, *15*, 2323–2343. [[CrossRef](#)]
13. Oh, Y. Semi-empirical model of the ensemble-averaged differential Mueller matrix for microwave backscattering from bare soil surfaces. *IEEE Trans. Geosci. Remote Sens.* **2002**, *40*, 1348–1355. [[CrossRef](#)]
14. Dubois, P.C.; van Zyl, J.; Engman, T. Measuring soil moisture with imaging radars. *IEEE Trans. Geosci. Remote Sens.* **1995**, *33*, 915–926. [[CrossRef](#)]
15. Wu, T.D.; Chen, K.S.; Shi, J.; Fung, A.K. A transition model for the reflection coefficient in surface scattering. *IEEE Trans. Geosci. Remote Sens.* **2001**, *39*, 2040–2050.
16. Fung, A.K.; Chen, K.S. An update on the IEM surface backscattering model. *IEEE Geosci. Remote Sens. Lett.* **2004**, *1*, 75–77. [[CrossRef](#)]
17. Chen, K.S.; Wu, T.D.; Tsay, M.K.; Fung, A.K. A note on the multiple scattering in an IEM model. *IEEE Trans. Geosci. Remote Sens.* **2000**, *38*, 249–256. [[CrossRef](#)]
18. Chen, K.S.; Wu, T.D.; Tsang, L.; Li, Q.; Shi, J.; Fung, A.K. Emission of rough surfaces calculated by the integral equation method with comparison to three-dimensional moment method simulations. *IEEE Trans. Geosci. Remote Sens.* **2003**, *41*, 90–101. [[CrossRef](#)]
19. Notarnicola, C.; Angiulli, M.; Posa, F. Soil moisture retrieval from remotely sensed data: Neural network approach *versus* Bayesian method. *IEEE Trans. Geosci. Remote Sens.* **2008**, *46*, 547–557. [[CrossRef](#)]
20. Said, S.; Kothyari, U.C.; Arora, M.K. ANN-based soil moisture retrieval over bare and vegetated areas using ERS-2 SAR data. *J. Hydrol. Eng.* **2008**, *13*, 461–475. [[CrossRef](#)]

21. Paloscia, S.; Pampaloni, P.; Pettinato, S.; Santi, E. A comparison of algorithms for retrieving soil moisture from ENVISAT/ASAR images. *IEEE Trans. Geosci. Remote Sens.* **2008**, *46*, 3274–3284. [[CrossRef](#)]
22. Pasolli, L.; Notarnicola, C.; Bruzzone, L. Estimating soil moisture with the support vector regression technique. *IEEE Geosci. Remote Sens. Lett.* **2011**, *8*, 1080–1084. [[CrossRef](#)]
23. Pasolli, L.; Notarnicola, C.; Bertoldi, G.; Chiesa, S.D.; Niedrist, G.; Bruzzone, L.; Tappeiner, U.; Zebisch, M. Soil moisture monitoring in mountain areas by using high-resolution SAR images: Results from a feasibility study. *Eur. J. Soil Sci.* **2014**, *65*, 852–864. [[CrossRef](#)]
24. Fung, A.K.; Li, Z.; Chen, K.S. Backscattering from a randomly rough dielectric surface. *IEEE Trans. Geosci. Remote Sens.* **1992**, *30*, 356–369. [[CrossRef](#)]
25. Rao, S.S.; Kumar, S.D.; Das, S.N. Modified dubois model for estimating soil moisture with dual polarized SAR data. *J. Indian Soc. Remote Sens.* **2013**, *41*, 865–872.
26. Sahebi, M.R.; Angles, J. An inversion method based on multi-angular approaches for estimating bare soil surface parameters from RADARSAT-1. *Hydrol. Earth Syst. Soc.* **2010**, *14*, 2355–2366. [[CrossRef](#)]
27. Chai, X.; Zhang, T.T.; Shao, Y.; Gong, H.Z.; Liu, L.; Xie, K.X. Modeling and mapping soil moisture of plateau pasture using RADARSAT-2 imagery. *Remote Sens.* **2015**, *7*, 1279–1299. [[CrossRef](#)]
28. Panciera, R.; Tanase, M.A.; Lowell, K.; Walker, J.P. Evaluation of IEM, Dubois and Oh radar backscatter models using airborne L-band SAR. *IEEE Trans. Geosci. Remote Sens.* **2014**, *52*, 4966–4979. [[CrossRef](#)]
29. Wagner, W.; Noll, J.; Borgeaud, M.; Rott, H. Monitoring soil moisture over the Canadian prairies with the ERS scatterometer. *IEEE Trans. Geosci. Rem. Sens.* **1999**, *37*, 206–216. [[CrossRef](#)]
30. Lievens, H.; Verhoest, N.E.C. Spatial and temporal soil moisture estimation from RADARSAT-2 imagery over Flevoland, The Netherlands. *J. Hydrol.* **2012**, *456–457*, 44–56. [[CrossRef](#)]
31. Jacome, A.; Bernier, M.; Chokmani, K.; Gauthie, Y.; Poulin, J.; de Sève, D. Monitoring volumetric surface soil moisture content at the La Grande Basin Boreal Wetland by radar multi polarization data. *Remote Sens.* **2013**, *5*, 4919–4941. [[CrossRef](#)]
32. Hornáček, M.; Wagner, W.; Sabel, D.; Truong, H.L.; Snoeij, P.; Hahmann, T.; Diedrich, E.; Doubková, M. Potential for high resolution systematic global surface soil moisture retrieval via change detection using Sentinel-1. *IEEE J. Sel. Top. Appl. Earth Obs. Remote Sens.* **2012**, *5*, 1303–1311. [[CrossRef](#)]
33. Notarnicola, C. A bayesian change detection approach for retrieval of soil moisture variations under different roughness conditions. *IEEE Geosci. Remote Sens. Lett.* **2014**, *11*, 414–418. [[CrossRef](#)]
34. Srivastava, H.S.; Patel, P.; Sharma, Y.; Navalgund, R.R. Large-area soil moisture estimation using multi-incidence-angle RADARSAT-1 SAR data. *IEEE Trans. Geosci. Remote Sens.* **2009**, *47*, 2528–2535. [[CrossRef](#)]
35. Baghdadi, N.; Cresson, R.; Pottier, E.; Aubert, M.; Zribi, M.; Jacome, A.; Benabdallah, S.A. Potential use for the C-band polarimetric SAR parameters to characterize the soil surface over bare agriculture fields. *IEEE Trans. Geosci. Remote Sens.* **2012**, *50*, 3844–3858. [[CrossRef](#)]
36. Bourgeau-Chavez, L.L.; Leblon, B.; Charbonneau, F.; Buckley, J.R. Evaluation of polarimetric Radarsat-2 SAR data for development of soil moisture retrieval algorithms over a chronosequence of black spruce boreal forests. *Remote Sens. Environ.* **2013**, *132*, 71–85. [[CrossRef](#)]
37. Pierdicca, N.; Castracane, P.; Pulvirenti, L. Inversion of electromagnetic models for bare soil parameter estimation from multifrequency polarimetric SAR data. *Sensors* **2008**, *8*, 8181–8200. [[CrossRef](#)]
38. Zribi, M.; Baghdadi, N.; Holah, N.; Fafin, O. New methodology for soil surface moisture estimation and its application to ENVISAT-ASAR multi-incidence data inversion. *Remote Sens. Environ.* **2005**, *96*, 485–496. [[CrossRef](#)]
39. Baghdadi, N.; Holah, N.; Zribi, M. Soil moisture estimation using multi-incidence and multi-polarization ASAR data. *Int. J. Remote Sens.* **2006**, *27*, 1907–1920. [[CrossRef](#)]
40. Hajnsek, I.; Jagdhuber, T.; Schön, H.; Papathanassiou, K.P. Potential of estimating soil moisture under vegetation cover by means of PolSAR. *IEEE Trans. Geosci. Remote Sens.* **2009**, *47*, 442–454. [[CrossRef](#)]
41. Jagdhuber, T.; Hajnsek, I.; Bronstert, A.; Papathanassiou, K.P. Soil Moisture Estimation Under low vegetation cover using a multi-angular polarimetric decomposition. *IEEE Trans. Geosci. Remote Sens.* **2013**, *51*, 2201–2215. [[CrossRef](#)]
42. Jagdhuber, T.; Hajnsek, I.; Papathanassiou, K.P. An iterative generalized hybrid decomposition for soil moisture retrieval under vegetation cover using fully polarimetric SAR. *IEEE J. Sel. Top. Appl. Earth Obs. Remote Sens.* **2015**, *8*, 3911–3922. [[CrossRef](#)]

43. ESA. Next ESA SAR Toolbox. Available online: <https://earth.esa.int/web/nest/downloads> (accessed on 8 May 2014).
44. Zribi, M.; Dechambre, M. A new empirical model to retrieve soil moisture and roughness from C-band radar data. *Remote Sens. Environ.* **2003**, *84*, 42–52.
45. Zribi, M.; Gorrab, A.; Baghdadi, N. A new soil roughness parameter for the modelling of radar backscattering over bare soil. *Remote Sens. Environ.* **2014**, *152*, 62–73. [[CrossRef](#)]
46. Vapnik, V. *The Nature of Statistical Learning Theory*; Springer-Verlag: New York, NY, USA, 1995.
47. Pasolli, L.; Notarnicola, C.; Bruzzone, L. Multi-objective parameter optimization in support vector regression: General formulation and application to the retrieval of soil moisture from remote sensing data. *IEEE J. Sel. Top. Appl. Earth Obs. Remote Sens.* **2012**, *5*, 1495–1508. [[CrossRef](#)]
48. Stamenkovic, J.; Ferrazzoli, P.; Guerriero, L.; Tuia, D.; Thiran, J.P. Joining a discrete radiative transfer Model and a kernel retrieval algorithm for soil Moisture estimation From SAR Data. *IEEE J. Sel. Top. Appl. Earth Obs. Remote Sens.* **2015**, *8*, 3463–3474. [[CrossRef](#)]
49. Mercer, J. Functions of Positive and negative type, and their connection with the theory of integral equations. *Philos. Trans. Roy. Soc. London Ser. A* **1909**, *209*, 415–446. [[CrossRef](#)]
50. Topp, G.C.; Davis, J.L.; Annan, A.P. Electromagnetic determination of soil water content: Measurements in coaxial transmission lines. *Water Resour. Res.* **1980**, *16*, 574–582. [[CrossRef](#)]
51. Paloscia, S.; Pettinato, S.; Santi, E.; Notarnicola, C.; Pasolli, L.; Reppucci, A. Soil moisture mapping using Sentinel-1 images: Algorithm and preliminary validation. *Remote Sens. Environ.* **2013**, *134*, 234–248. [[CrossRef](#)]
52. Ulaby, F.T.; Moore, R.K.; Fung, A.K. *Microwave Remote Sensing: Active and Passive, Vol. III: Scattering and Emission Theory, Advanced Systems and Applications*; Artech House: Dedham, MA, USA, 1986.
53. Baghdadi, N.; Aubert, M.; Zribi, M. Use of TerraSAR-X Data to Retrieve Soil Moisture over Bare Soil Agricultural Fields. *IEEE Geosci. Remote Sens. Lett.* **2012**, *9*, 512–516. [[CrossRef](#)]
54. Baghdadi, N.; Holah, N.; Dubois, P.; Prévot, L.; Hosford, S.; Chanzy, A.; Dupuis, X.; Zribi, M. Discrimination potential of X-band polarimetric SAR data. *Int. J. Remote Sens.* **2004**, *25*, 4933–4942. [[CrossRef](#)]
55. Baghdadi, N.; Zribi, M.; Loumagne, C.; Ansart, P.; Paris Anguela, T. Analysis of TerraSAR-X data and their sensitivity to soil surface parameters over bare agricultural fields. *Remote Sens. Environ.* **2008**, *112*, 4370–4379. [[CrossRef](#)]
56. Aubert, M.; Baghdadi, N.; Zribi, M.; Douaoui, A.; Loumagne, C.; Baup, F.; el Hajj, M.; Garrigues, S. Analysis of TerraSAR-X data sensitivity to bare soil moisture, roughness, composition and soil crust. *Remote Sens. Environ.* **2011**, *115*, 1801–1810. [[CrossRef](#)]
57. Srivastava, H.S.; Patel, P.; Manchanda, M.L.; Adiga, S. Use of multi-incidence angle RADARSAT-1 SAR data to incorporate the effect of surface roughness in soil moisture estimation. *IEEE Trans. Geosci. Remote Sens.* **2003**, *41*, 1638–1640. [[CrossRef](#)]
58. Pasolli, L.; Notarnicola, C.; Bruzzone, L.; Bertoldi, G.; Chiesa, S.D.; Niedrist, G.; Tappeiner, U.; Zebisch, M. Polarimetric RADARSAT-2 imagery for soil moisture retrieval in alpine areas. *Can. J. Remote Sens.* **2011**, *37*, 535–547. [[CrossRef](#)]



© 2015 by the authors; licensee MDPI, Basel, Switzerland. This article is an open access article distributed under the terms and conditions of the Creative Commons Attribution (CC-BY) license (<http://creativecommons.org/licenses/by/4.0/>).